Reviewed research article

Deglacial and Holocene sediment distribution in Hestvatn, South Iceland, derived from a seismic and multibeam survey

Hrafnhildur Hannesdóttir[1], Áslaug Geirsdóttir[1], Gifford H. Miller[2], William Manley[2] and Nigel Wattrus[3]

[1]*Institute of Earth Sciences and Department of Earth Sciences, University of Iceland, Askja, Sturlugata 7, 101 Reykjavík, Iceland*

[2]*Institute of Arctic and Alpine Research and Department of Geological Sciences, University of Colorado, 1560 30th Street, Boulder, CO 80303*

[3]*Large Lakes Observatory and Department of Geological Sciences, University of Minnesota, Duluth, Duluth, MN 55812, USA*

hrafnha@hi.is

Abstract — *More than 100 km of seismic reflection profiles together with a new multibeam survey of the sediment fill in lake Hestvatn, South Iceland, reveal two sub-basins filled with up to 44 m of deglacial and Holocene sediment. The chronology is constrained by geochemically characterized tephra layers and radiocarbon dates on marine molluscs. The Vedde Ash and Saksunarvatn Ash provide key chronological control for the deglacial sediment. Five seismic units are tied to the lithostratigraphy of sediment cores obtained from the two basins. The seismic units reveal major changes from glacial, to glacial-marine, to lacustrine sedimentary environments. Isopach maps of the seismic units document changes in the primary sediment depocenters, sedimentation rates and sediment delivery through time. The Vedde Ash, found only in glacial-marine sediment in the southern basin, suggests that during the Younger Dryas the northern basin of Hestvatn was occupied by an outlet glacier from the main Icelandic Ice Sheet that calved into a marine embayment. A high-resolution multibeam bathymetric survey reveals multiple shallow ridges between the two sub-basins of Hestvatn, which presumably acted as a pinning point for the calving glacier. During and after the retreat of the glacier and isolation of the lake basin, lacustrine sediments were mainly deposited via northern and northwesterly inlets, resulting in higher sedimentation rates in the north basin compared to the south basin. Early in the lacustrine phase repeated turbidites were deposited, interpreted to originate in glacial outburst floods (jökulhlaups) following a retreating ice-margin in central Iceland.*

INTRODUCTION

Most studies of the deglaciation of Iceland reveal a dynamic Iceland Ice Sheet that responded rapidly to changes in solar radiation, ocean currents, and sea level. Seismic surveys and sediment core studies of the Iceland Shelf and glacial geological mapping on land show evidence for a rapid but step-wise deglaciation, associated with changes in relative sea level (Syvitski *et al.*, 1999; Andrews *et al.*, 2000; Jennings *et al.*, 2000; Eiriksson *et al.*, 2000; Geirsdóttir *et al.*, 2002; Andrews and Helgadóttir, 2003; Geirsdóttir *et al.*, 2009, Ingólfsson and Norðdahl, 1994, 2001). Because isostatic recovery exceeded sea level rise during deglaciation (Norðdahl and Pétursson, 2005) most

coastal sites contain evidence for fluctuating tidewater glacier termini occupying paleo fjords and bays (e.g., Geirsdóttir *et al.*, 1997; Geirsdóttir *et al.*, 2000; Geirsdóttir *et al.*, 2007; Norðdahl and Pétursson, 2005; Hannesdóttir, 2006). The deglaciation in Iceland also coincided with an increase in volcanic activity (Jakobsson *et al.*, 1978; Sigvaldason *et al.*, 1992; Jull and McKenzie, 1996; Sinton *et al.*, 2005). Subglacial lakes and subaerial ice-dammed lakes drained in repeated jökulhlaups (e.g. Kjartansson, 1964; Tómasson, 1993) that delivered large pulses of sediment to lake basins and the marine environment (Geirsdóttir *et al.*, 1997; Lacasse *et al.*, 1998; Geirsdóttir *et al.*, 2000; Hannesdóttir, 2006).

The history of glacier growth and retreat in Iceland during the last deglaciation and the Holocene is mostly based on morphological studies of glacial features and palynological studies of peat sections and raised shorelines/terraces showing the step-wise retreat/advance of the main ice sheet through the Allerød/Bølling, Younger Dryas and the PreBoreal times (Rundgren *et al.*, 1997; Ingólfsson and Norðdahl, 1994; Norðdahl and Pétursson, 2005). The Búði moraine complex in South Iceland is probably the strongest evidence for this step-like retreat (or advance) of the main ice sheet and the associated series of relative sea-level changes. Although most ^{14}C dates indicate a Preboreal age for their formation (Hjartarson and Ingólfsson, 1988), a recent study of the moraine complex, supported by studies on sediment cores obtained from Hestvatn, a lake located 25 km in front of the moraines, suggests parts of the moraines were formed during Younger Dryas time when the southern lowlands were a marine embayment (Geirsdóttir *et al.*, 1997, Geirsdóttir *et al.*, 2000; Harðardóttir *et al.*, 2001a). A tephra layer geochemically identified as the Vedde Ash (11.8 ka (calibrated years before present), Grönvold *et al.*, 1995) found in Hestvatnt's marine deposits underlying lacustrine sediment confirms local deglaciation prior to Younger Dryas time (Geirsdóttir *et al.*, 1997, 2000; Harðardóttir *et al.*, 2001a; Hannesdóttir, 2006).

In this paper we examine the sedimentation pattern in Hestvatn from before the deposition of the Vedde Ash to present day based on over 100 km of seismic reflection profiles of the sediment fill, a new high-resolution multibeam survey, and sediment cores. Isopach maps built on the re-evaluation of the seismic survey indicate striking shifts in sediment source and depositional environments from the earliest phase of sediment infill and after isolation of the lake basin. Hestvatn is ideally positioned to provide information on the shift from glacial to interglacial regime, isostatic rebound, and marine to terrestrial environment. Efficient glacial erosion of the soft bedrock of Iceland has resulted in high sedimentation rates, approaching 1 m ka^{-1} for most of the Holocene. Seismic reflection surveys on the lake, studies of new sediment cores and underlying marine sediment provide essential information on sediment distribution, thickness and depositional processes where acoustic properties allow tracing of seismic units within the lake. A change in depositional environment is seen from glacial to glacial marine and lacustrine sedimentation with episodic turbidite formation concurrent to isostatic uplift and catastrophic release of meltwater from a retreating ice margin.

PHYSICAL SETTING

Hestvatn (6.8 km^2) is situated 49.5 m a. s. l. in the lowlands of South Iceland, seaward of the Búði moraines (Figure 1). Basalt and hyaloclastite constitute the main rock types of the Hestvatn basin (Tómasson, 1961). Mt. Hestfjall (319 m a. s. l.), partly formed subglacially, shows classic table mountain characteristics, with glacial striations on top, dominantly a southwesterly direction, but westerly and southerly striations exist as well (Tómasson, 1961). Marine terraces are preserved on the western side of the mountain, at 94 m, 75 m and 60 m a. s. l. (Kjartansson, 1939; Tómasson, 1961) and an excavation on the south shore of the lake reveals a sandy gravelly marine delta (Figure 1b).

The lake basin has been subject to both tectonic activity as well as glacial erosion, resulting in a N-S orientation, with two >60 m deep basins, separated by a deep but narrow (200 m wide) channel (Figure 2). In the present regime inflow is limited to a few small creeks on the northern side of the lake. Slauka, formerly known as Hestlækur is the only outflow (Fig-

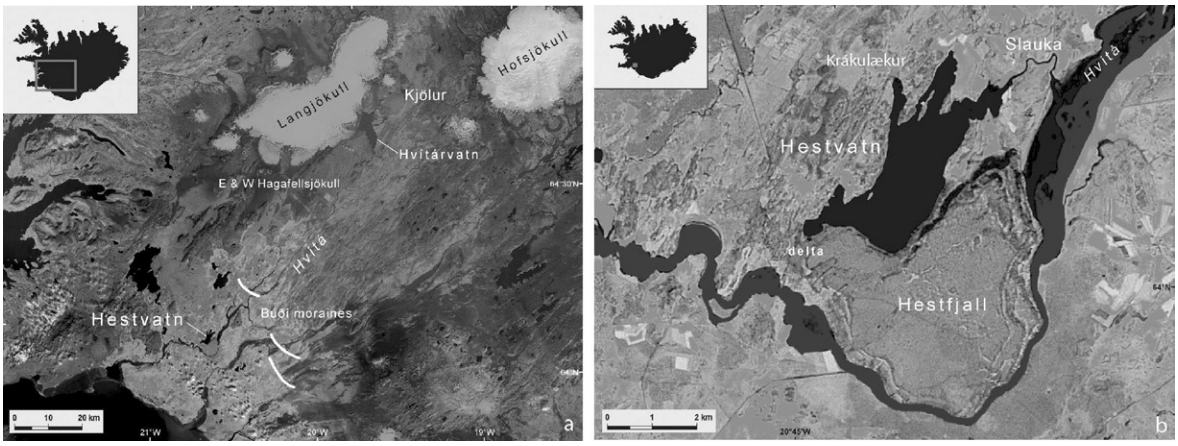

Figure 1. Landsat images of the research area. a. River Hvítá drains Hvítárvatn by Langjökull, and flows east of Hestvatn. Simplified configuration of the Búdi moraines is drawn. Two of the outlet glaciers of Langjökull, E and W Hagafellsjökull are indicated. b. River Slauka is the only outflow of Hestvatn, but when water level of Hvítá is high, water is diverted into Hestvatn via Slauka. Location of ice-proximal delta on the southwest shore of Hestvatn is shown. – *Gervitunglamyndir af rannsóknarsvæðinu. Hvítá rennur úr Hvítárvatni við Langjökul og austan og suður með Hestvatni. a. Einfölduð mynd af Búðaröðinni. b. Slauka er eina útfall Hestvatns. Þegar vatnsstaða Hvítár er há flæðir inn í vatnið um Slauku. Suðvestur af Hestvatni er þykkir bunkar af sjávarseti sem líklega hafa hlaðist upp framan við jökul.*

ure 2). However, the glacial river Hvítá flows occasionally into the lake via Slauka, either when ice-dams form on the river or increased glacial meltwater, caused by spring floods, or surges of East or West Hagafellsjökull (Figure 1a), outlet glaciers of the ice cap Langjökull (e.g. Sigbjarnarson, 1976). Inflow from Hvítá is known to take place on an approximately bi-decadal timescale (Harðardóttir *et al.*, 2001a).

METHODS

A seismic survey was conducted on Hestvatn in 1994 (Harðardóttir *et al.*, 2001a). Over 100 km of seismic reflection data were collected from the survey boat Bláskel, equipped with a Geopulse Boomer system. The system operated at 175 J and the data were filtered for frequencies between 0.75 kHz and 20 kHz. The boat was positioned with a Trimble 4000 DS Differential GPS system with a $\pm$20 m resolution. Sediment thickness, calculated using freshwater sound velocity of 1465 m s^{-1}, represents a minimum thickness. Seismic lines were spaced approximately 100 m apart along SSW-NNE lines, but more sparsely distributed E-W lines were surveyed (Figure 2a). Black and white lines in Figure 2a indicate the track of the boat and surveyed profiles, however, in a few places the equipment gave unsuccessful results. Harðardóttir *et al.* (2001a) analyzed the seismic profiles but here we extend the survey and add ArcGIS procedures to more thoroughly analyze the data.

The seismic profiles were digitized and the seismic data processed using Geographic Information System (GIS) for further analysis. Raster and vector datasets were assembled with a consistent projection (Iceland Lambert) and datum (ISNET93/WGS84). Datasets included point shapefiles for bathymetry and thicknesses of sedimentary units, raster versions of 1:50,000 maps of the Hestvatn area (sheets 1712-IV and 1713-III) from the National Land Survey of Iceland, the Hestvatn shoreline, shapefiles for core locations and seismic transects, Landsat 7 satellite images of the research area.

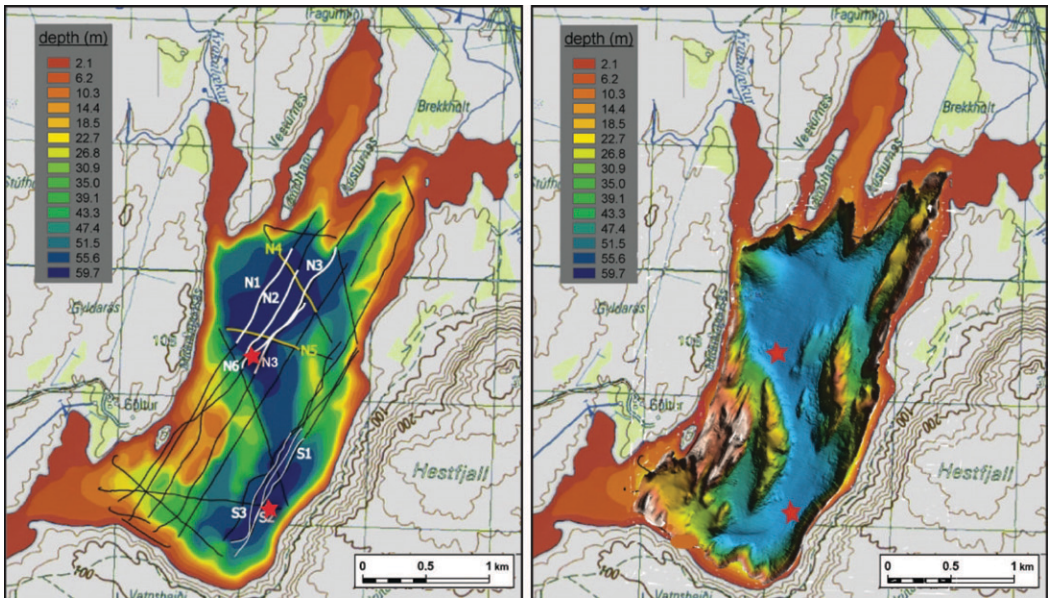

Figure 2. a. Bathymetry of Hestvatn, seismic profiles and core locations. Black lines indicate tracks of seismic profiles, only white line profiles are shown in figures 3 and 4b. b. Multibeam bathymetric map of lake floor of Hestvatn superimposed on the original bathymetric map to provide coverage in shallow water. Subareal map published with permission from the National Land Survey of Iceland. – *a. Dýptarkort Hestvatns ásamt siglingalínum endurvarpsmælinga (gögn eftir hvítum línum er sýnd á myndum 3 og 4). Hvítir punktar sýna staðsetningu kjarna sem teknir voru sumarið 2003. b. Fjölgeislamælingar af botni Hestvatns leiða í ljós landslag á grunnum svæðum vatnsins. Kort birt með leyfi Landmælinga Íslands.*

A detailed bathymetric map was compiled by combining water depth calculations from the seismic survey, and scanned and georectified bathymetric map made with echo sounder measurements by the Hydrological Service Division of the Energy Authority in Iceland (Rist, 1975). Isopach maps of the seismic units were created by interpolation, both for the lake's two sub-basins and the whole lake. The number of points varied depending on seismic unit (ranging from 1200 to 4600 points). The interpolation was limited to areas of 180 m of the data points, with resulting 3 m grid cell spacing. Isopach maps for the lake's two sub-basins were created, as well as isopach maps for the whole lake. Paleobathymetry maps were created, subtracting sediment thickness from the modern bathymetry. The mean thickness and volume for the seismic units was calculated for the two sub-basins as well as for the whole lake.

DOSECC's GLAD200 core rig (http://www.-dosecc.org/), equipped with ODP-style coring tools was used to recover over 20 m long cores at 60 m water depth in Hestvatn in the summer of 2003. Sediment cores from Hestvatn obtained in 1994 and 1995 (Harðardóttir *et al.*, 2001a, 2001b) and the seismic survey guided the selection of the new core sites. Four new cores were obtained from Hestvatn, a set of duplicate cores from each sub-basin (Figure 2), with a vertical offset of approximately 1.5 m (Table 1). Each core segment is approximately 3 m long and 6.2 cm in diameter. Additionally surface cores (Glew, 1991) were recovered from each location, in order to retrieve the water/sediment interface at the core sites. The chronology of the cores is based on tephrochronology and radiocarbon dating of marine molluscs (Table 2). Seismic units are identified by comparison of the seismic profiles and the core lithology.

Table 1. The GLAD4-HST03 cores and their position in UTM (Hjörsey datum). – *Staðsetning GLAD4-HST03 kjarnanna í UTM hnitum.*

cores	UTM N	UTM E
GLAD4-HST03-1A	7098130	514226
GLAD4-HST03-1C and 1D	7098122	514204
GLAD4-HST03-2A and 2B	7099341	514063

In 2005, a Reson Seabat 8101 multibeam sonar system was used to acquire a high resolution bathymetric survey on Hestvatn. This system operates at 240 kHz and uses 101 1.5 degree beams to measure bathymetry. The system's range resolution is 1.25 cm. Its lateral resolution is dependent on water depth and the number of beams retained in the processed data. The data were acquired on transects spaced at 75 m intervals ensuring that the survey achieved 100% coverage of the lake floor.

Information on the survey vessel's motion and position was obtained from an Applanix POS MV/320 motion sensing and positioning system. This system measures vessel motion to an accuracy of <0.05 degrees and position to <1 m horizontally and <25 cm vertically. Differential corrections for the positioning system were sent via a radio link, from a temporary base station established on the lakeshore.

The speed of sound in water varies with temperature, pressure and salinity. Uncorrected these variations would produce refraction artifacts in the data. To correct these, profiles of the speed of sound in the water column were collected periodically with a SVPlus Sound Velocimeter. The collected bathymetry data were processed using CHARIS HIPS. The processing removes outliers from the data and applies appropriate corrections for vessel motion and ray bending due to sound velocity variations. The processed data were used to produce a high-resolution bathymetric map that was gridded at an interval of 2–4% of the maximum water depth.

RESULTS

Interpretation of seismic survey linked to sediment core lithostratigraphy

The bathymetric map together with the new multibeam bathymetric data reveals two approximately 60 m deep sub-basins, the southern basin and the northern basin (Figure 2). The two sub-basins are connected by a 200 m wide channel at >50 m water depth, but flanked by two N-S lying elongated ridges at water depths of less than 10 m and with smaller N-S lying "drumlin like" ridges varying in height between 4 and 7 m, occupying the channel floor. The bathymetry shows steep bedrock walls adjacent to the two relatively deep and flat sub-basins, and shallow coves on the southern and northern side of the lake. The deepest parts of the lake lie approximately 10 m below present day sea level. The multibeam images reveal several fan-like structures; in the north as a continuation of Krákulækur creek; in front of the shallow cove in the southwest of the lake and into the deep southern basin, and along the steep bedrock walls on the eastern side of the lake (Figure 2b).

Locations of seismic reflection lines illustrating the two sub-basins are shown in Figure 2a. A series of northwest lying seismic profiles lined up from west to east within each sub-basin are shown in Figures 3 (north basin) and 4 (south basin). The seismic survey reveals variable distribution of sediment within the lake. The two sub-basins act as the main depositional centers with maximum sediment thickness of 44 m and average thickness of 27 ± 5 m, whereas on ridges and elsewhere sediment thickness is on average 5 ± 5 m (Figure 5). Sediment on the sidewalls is much thinner, in some places absent. Comparison of the seismostratigraphic units and lithology of the sediment cores allowed identification of three main seismic units (I, II and III), and all but the bottom unit I, are traceable between the two sub-basins (Figures 3 and 4). The seismic units represent periods of similar sedimentation environments, but their subdivisions have no time significance, except for seismic unit III. Chronological control is poorer for the lower two seismic units in the two sub-basins than for the upper part of the sedimentary record.

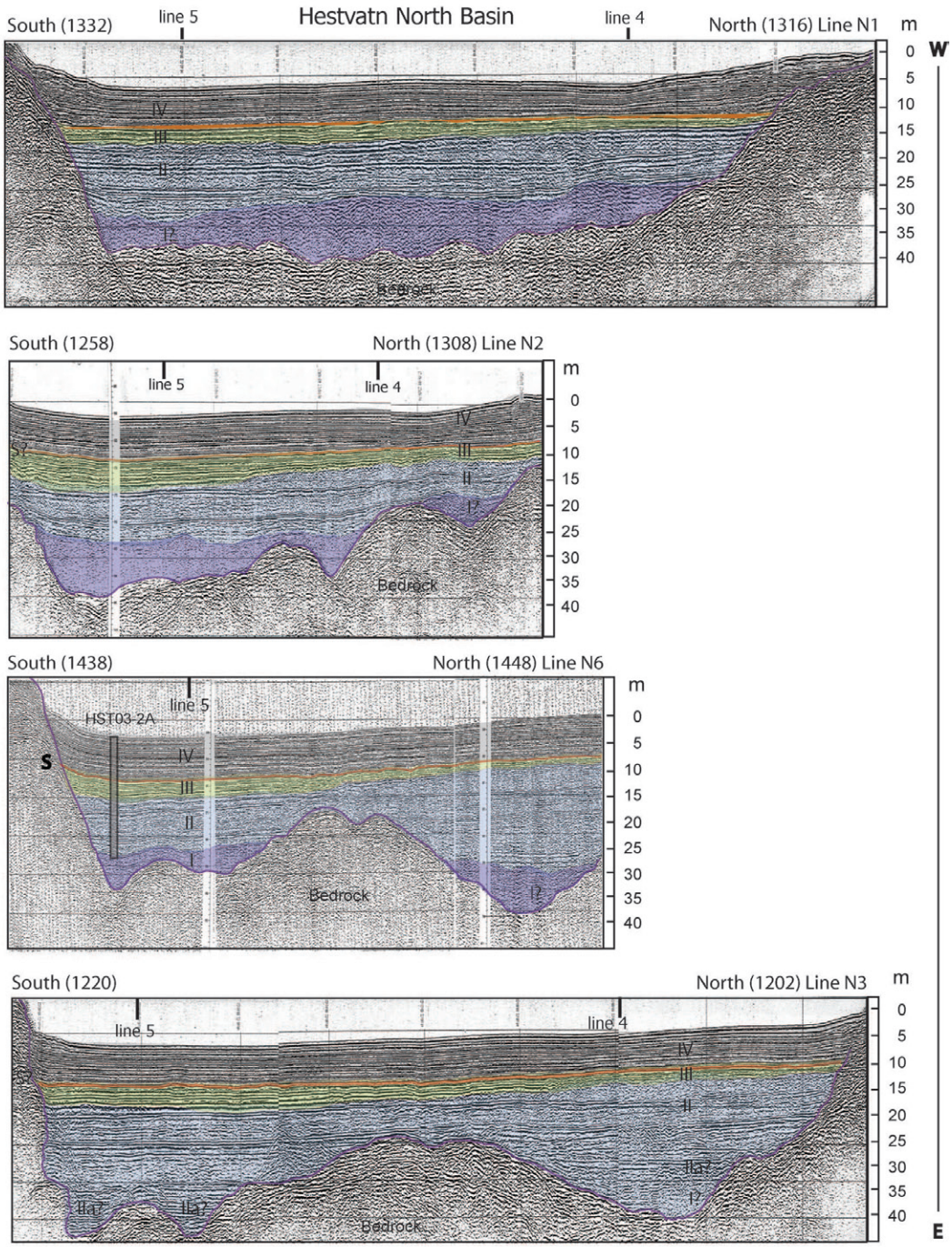

Figure 3. Seismic profiles from the North Basin (Figure 2a). Seismic unit I is only found in this basin as discontinuous hummocks in places, see Line 3. The orange line represents the Saksunarvatn Ash (S).

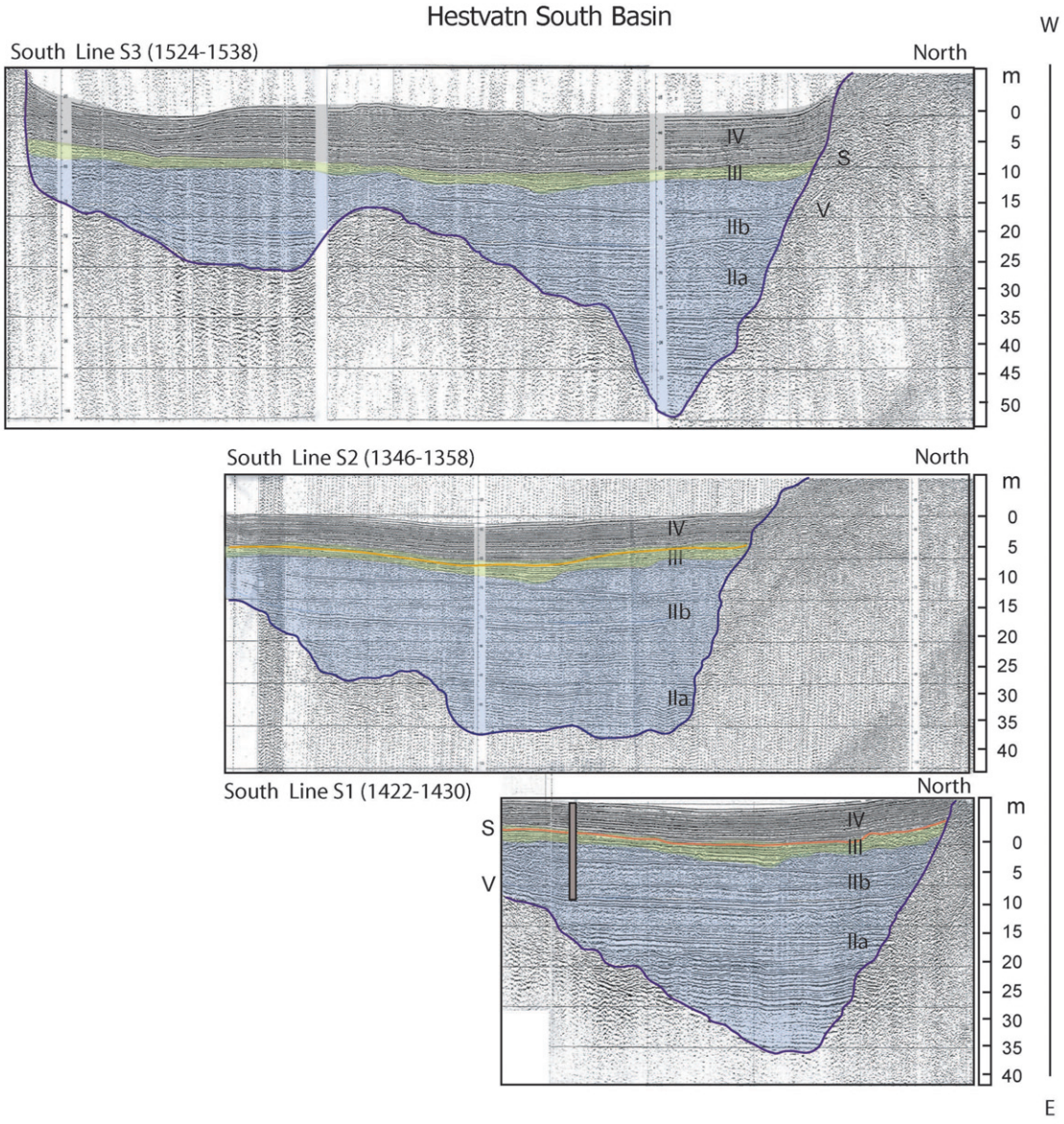

Figure 4. Seismic profiles from the South Basin where total sediment infill is thickest. The orange line represents the Saksunarvatn Ash (S). The Vedde Ash (V) is indicated with the red line on Line S1. – *Endurvarpslínur úr norðurdæld (3. mynd) og suðurdæld (4. mynd) vatnsins þar sem setlög eru þykkust. Endurvarpseining I er einungis í norðurhluta vatnsins og myndar ósamfelldar mishæðir líkt og sjá má á línu N3. Appelsínugul lína táknar Saksunarvatns gjóskulagið (S) í báðum dældum, en Vedde gjóskulagið er litað rautt á línu S1 og finnst einungis í suðurhluta vatnsins.*

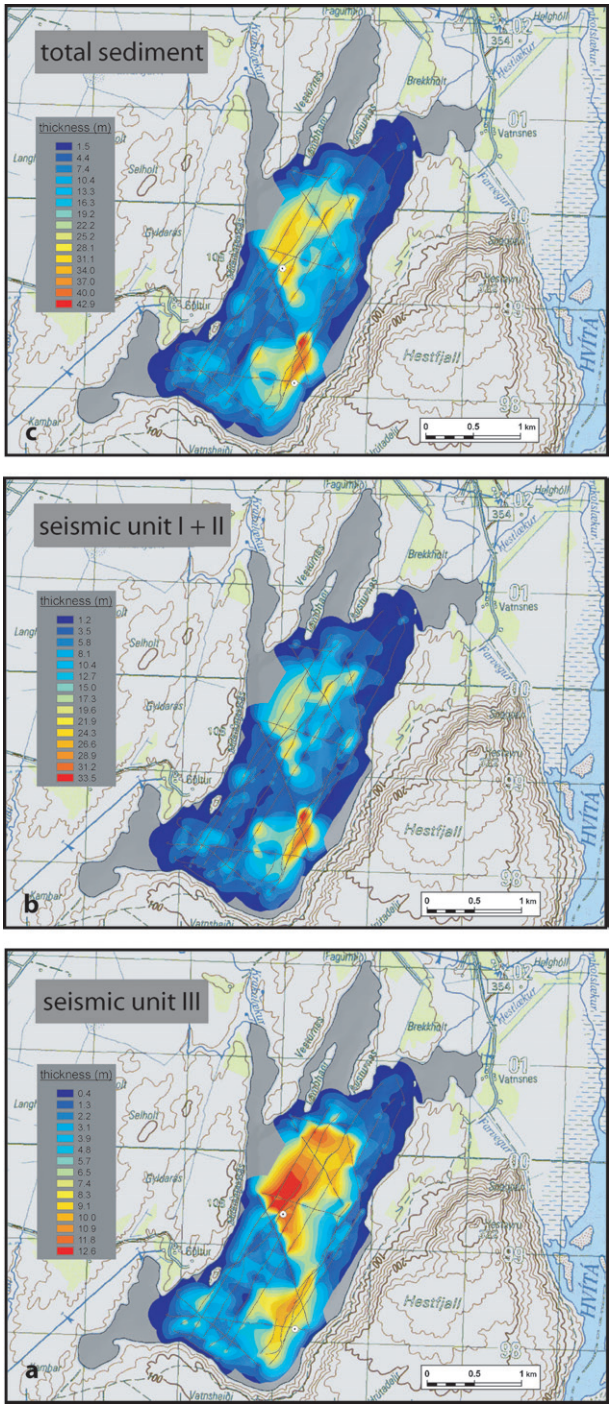

Figure 5. Isopach maps of the whole lake made by interpolation of seismic data. a. Total sediment infill of Hestvatn deposited over the last 12,000 years. b. Isopach map of seismic unit I + II(a+b). c. Isopach map of seismic unit III(a+b). Subareal map published with permission from the National Land Survey of Iceland. – *Jafnþykktarkort af öllu vatninu reiknað út frá endurvarpsgögnum. a. Set sem sest hefur til á síðustu 12.000 árum. b. Jafnþykktarkort af einingum I+II(a+b). c. Jafnþykktarkort af einingu III(a+b). Kort birt með leyfi Landmælinga Íslands.*

Table 2. The chronology of the Hestvatn record of the GLAD4-HST03 cores is based on dated tephra layers and radiocarbon dates of humic acid fraction of total dissolved organic carbon (h), microfossils (m) and marine molluscs (s). A 400-year reservoir correction is used for the marine carbonate ages according to results of Sveinbjörnsdóttir *et al.* (1998) (corrected dates marked with *). Calibrated ages were obtained using the CALIB program Rev. 4.4.2 (Stuiver and Reimer, 1993; Stuiver *et al.*, 1998). Calibrated ages are presented with 1s and 95% confidence level. Date R = radiocarbon dated, I = interpolated radiocarbon date, W = wiggle-match of radiocarbon dates, IC = ice-core age. H = historical account. – *Aldursákvarðanir fyrir Hestvatnssetið byggjast á þekktum gjóskulögum og geislakolsmælingum á skeljum, með 400 ára aldursleiðréttingu sjávar, samanber niðurstöður Árnýjar E. Sveinbjörnsdóttur og fl. (1998). Leiðréttur aldur (merktur *), var fenginn með CALIB forritinu Rev. 4.4.2 (Stuiver og Reimer, 1993; Stuiver og fl. 1998).*

Hestvatn core section	cum. depth (cm)	sample number /tephra	radiocarbon age (^{14}C yr BP)	cal. age (yr BP)	date type	Reference
NORTH BASIN CORE						
GLAD4-HST03-2A-1H-1	50	NSRL-13571 (h)	1820±15	1764±32	R	Hannesdóttir, 2006
GLAD4-HST03-2A-1H-1	109	K-1500 tephra	X	460	H	Þórarinsson, 1975
GLAD4-HST03-2A-1H-1	173	NSRL-13468 (m)	1750±30	1660±48	R	Hannesdóttir, 2006
GLAD4-HST03-2A-1H-2	219	Vö tephra	871±2 AD	1080±2	IC	Grönvold *et al.*, 1995
GLAD4-HST03-2A-1H-2	231	NSRL-13741 (h)	2020±20	1963±29	R	Hannesdóttir, 2006
GLAD4-HST03-2A-2H-1	349	KE tephra[1]	2850±10	2967±24	I	Róbertsdóttir, 1992
GLAD4-HST03-2A-2H-1	349	KE tephra[2]	x	2914±104	I	Hannesdóttir, 2006
GLAD4-HST03-2A-2H-1	357	NSRL-13612 (h)	3910±15	4351±49	R	Hannesdóttir, 2006
GLAD4-HST03-2A-2H-1	360	H3 tephra	2880±35	3066±108	R	Dugmore *et al.*, 1995
GLAD4-HST03-2A-2H-1	393	KN tephra[1]	3300±100	3523±118	I	Róbertsdóttir, 1992
GLAD4-HST03-2A-2H-1	393	KN tephra[2])	x	3444±68	I	Hannesdóttir, 2006
GLAD4-HST03-2A-2H-1	458	NSRL-13501 (h)	4870±25	5615± 25	R	Hannesdóttir, 2006
GLAD4-HST03-2A-2H-1	464	H4 tephra	3830 ±15	4260±20	W	Dugmore *et al.*, 1995
GLAD4-HST03-2A-2H-2	555	T tephra	x	6100±100	I	Jóhannsdóttir, 2007
GLAD4-HST03-2A-2H-2	562	NSRL-13573 (h)	6000±20	6810±52	R	Hannesdóttir, 2006
GLAD4-HST03-2A-2H-2	571	A/A-1 tephra	5415	6300±100	I	Jóhannsdóttir, 2007
GLAD4-HST03-2A-2H-2	593	A/A-2 tephra	5785	6700±100	I	Jóhannsdóttir, 2007
GLAD4-HST03-2A-2H-2	604	A/A-3 tephra	5893	6800±100	I	Jóhannsdóttir, 2007
GLAD4-HST03-2B-3H-2	615	A/A-4 tephra	6120	7100±100	I	Jóhannsdóttir, 2007
GLAD4-HST03-2B-3H-2	628	SILK A8 tephra	6400	7300±100	I	Jóhannsdóttir, 2007
GLAD4-HST03-2B-3H-2	657	SILK A9	6600	7500±100	I	Jóhannsdóttir, 2007
GLAD4-HST03-2A-3H-1	668	NSRL-13574 (h)	7535±20	8361±15	R	Hannesdóttir, 2006
GLAD4-HST03-2A-3H-1	723	ThB-1 tephra	7330	8550±100	I	Jóhannsdóttir, 2007
GLAD4-HST03-2A-3H-1	724	ThH-1 tephra	7380	8600±100	I	Jóhannsdóttir, 2007
GLAD4-HST03-2A-3H-1	729	ThB-2 tephra	7445	8700±100	I	Jóhannsdóttir, 2007
GLAD4-HST03-2A-3H-1	736	A/B-1 tephra	7795	8950±100	I	Jóhannsdóttir, 2007
GLAD4-HST03-2A-3H-1	751	ThE-1 tephra	8015	9100±100	I	Jóhannsdóttir, 2007
GLAD4-HST03-2A-3H-1	752	NSRL-13502 (h)	8870±45	10,029±120	R	Hannesdóttir, 2006
GLAD4-HST03-2A-3H-2	792	Saksunarvatn tephra	9000	10,180±60	IC	Grönvold *et al.*, 1995
GLAD4-HST03-2A-3H-2	875	NSRL-13742 (h)	9665±35	11,029±139	R	Hannesdóttir, 2006
GLAD4-HST03-2A-4H-2	1130	NSRL-13744 (h)	9135±20	10,292 ±68	R	Hannesdóttir, 2006
GLAD4-HST03-2A-5H-3	1417	NSRL-13472 (s)	*9860±60/ 10,260±60	11,219±122	R	Hannesdóttir, 2006
GLAD4-HST03-2A-9H-1	2228	NSRL-13473 (s)	*9900±65/ 10,300±65	11,238±120	R	Hannesdóttir, 2006

Table 2. cont.

Hestvatn core section	cum. depth (cm)	sample number /tephra	radiocarbon age (^{14}C yr BP)	cal. age (yr BP)	date type	Reference
SOUTH BASIN CORE						
GLAD4-HST03-1A-1H-2	109	K-1500 tephra	360	460	H	Þórarinsson, 1975
GLAD4-HST03-1A-1H-2	192	Vö tephra	871±2 AD	1080±2	IC	Grönvold *et al.*, 1995
GLAD4-HST03-1A-1H-2	240	KE tephra	2850±10	2975±60	I	Róbertsdóttir, 1992
GLAD4-HST03-1A-H-2	248	H3 tephra	2880±30	3066±108	R	Dugmore *et al.*, 1995
GLAD4-HST03-1A-1H-2	263	KN tephra	3300±100	3555±120	I	Róbertsdóttir, 1992
GLAD4-HST03-1A-2H-1	306	H4 tephra	3830 ±10	4260±20	W	Dugmore *et al.*, 1995
GLAD4-HST03-1A-2H-1	334	T tephra	5765±55	6100±100	I	Jóhannsdóttir, 2007
GLAD4-HST03-1A-2H-1	427	Th-B1 tephra	7380	8600±100	I	Jóhannsdóttir, 2007
GLAD4-HST03-1A-2H-2	486	Saksunarvatn tephra	9000	10,180±60	IC	Grönvold *et al.*, 1995
GLAD4-HST03-1A-3H-1	627	AA59081 (s)	9925±56/ 9525±56	10,599±236	R	Hannesdóttir, 2006
GLAD4-HST03-1C-3H-2	825	AA59080 (s)	*9684±55/ 10,084±55	10,901±260	R	Hannesdóttir, 2006
GLAD4-HST03-1A-4H-1	926	AA59079 (s)	*9715±54/ 10,115±54	10,994±180	R	Hannesdóttir, 2006
GLAD4-HST03-1A-5H-1	1251	Vedde tephra	10,300	11,980±80	IC	Grönvold *et al.*, 1995
GLAD4-HST03-1A-5H-1	1316	AA59078 (s)	*9992±55/ 10,392±55	11,445±233	R	Hannesdóttir, 2006

Core HST03-2A obtained from the north basin lies on line N6 (Figure 3) - and core HST03-1A from the south basin on line S1 (Figure 4). Sediment core HST03-2A penetrated 23 m of sediment, with near complete sediment recovery, halting on the lowermost transparent seismic unit I. Sediment core HST03-1A penetrated 15 m of sediment, into sub-unit IIb, which consists of silty sediment interbedded with sandy-gravelly sediments and shell fragments. The sandy-gravelly section was not penetrable, leaving approximately 20 m of unrecovered sediment from the south basin core site.

The chronology of the cores is based on tephrochronology and radiocarbon dating of marine molluscs (Table 2). The two most widely distributed and recognized tephra layers in the North Atlantic, the Vedde Ash (11.8 ka) and the Saksunarvatn Ash (10.2 ka) provide key chronological control for the deglacial sediments (Grönvold *et al.*, 1995). The Vedde Ash (5 cm thick), is found at 12.5 m depth in core HST03-1A in the south basin (Figure 4), but is not present in the duplicate cores from the north basin. Vedde was also identified on x-radiographs (Hannesdóttir, 2006; Jóhannsdóttir, 2007). Microprobe analyses made on the tephra layer confirmed its origin as the Vedde Ash and its two phase appearance indicates primary fallout (Jóhannsdóttir, 2007). The age model for the marine section is not constrained by tephrochronology (apart from Vedde Ash), but depends on ^{14}C dates on marine molluscs, which are in chronological order. In core HST03-1A a date of 11,445±233 ka, is found 50 cm below the Vedde Ash, hence the upper limit of this date is 73 cal. years younger than the accepted age of the Vedde Ash.

A reservoir age of 400 years is used for the mollusc dates. The radiocarbon dates are affected by ^{14}C plateaux (Becker *et al.*, 1991; Kromer and Becker, 1993; Lowe and Walker, 2000) and as such have their limitations. Studies in the North Atlantic (i.e. Bard *et al.*, 1994; Haflidason *et al.*, 1995; Jennings *et al.*, 2000) indicate that a higher ocean reservoir correction might be needed for the late glacial/Holocene transition period than for younger intervals. Sveinbjörnsdóttir *et al.* (1998) compared ^{14}C dates of

foraminifera and molluscs from the 1995 Hestvatn cores, with the age of the Vedde Ash, and confirmed a reservoir age of 400 years at this location; low δ^{13}C values of the foraminifera and molluscs indicate that the site was greatly influenced by freshwater during the Younger Dryas chronozone.

The uppermost part of the record is based on diagnostic tephra layers correlated between sediment cores from 3 lakes in Iceland (Table 2; Jóhannsdóttir, 2007). Comparison of the humic acid dissolved organic carbon (HA-DOC) ^{14}C dates with the tephrochronology of core HST03-2A reveals that most radiocarbon dates are too old, and they are therefore not considered for chronological control (Hannesdóttir, 2006).

Seismic unit I is only found in the north basin and has acoustically chaotic appearance with variable relief and irregular, faint or no internal reflectors (Figure 3). Its thickness varies from 1 to a maximum of 10 m and forms in places discontinuous hummocks as seen in line N3 (Figure 3). Core HST03-2A sampled the top of this seismic unit, revealing an overconsolidated diamicton with silty matrix and pebbles. Difficulties were experienced penetrating these sediments during coring.

Seismic unit II (both a and b) is 16 m thick on average, with a maximum thickness of >25 m and is considerably thicker in the south basin than in the northern basin (Figures 3 and 4 and Table 3). Seismic subunit IIa forms the basal seismic unit in the south basin (Figure 4) and shows strong multiple reflectors, which grade into layers of strong internal reflectors interbedded with more chaotic layers in sub-unit IIb. This subunit IIa fills in the uneven basal topography of the underlying seismic unit I in the north basin, especially in seismic lines N1, N3 and N6, thereby smoothing out the basin sediment surface. Cores HST03-1A and 2A did not capture any of the sediment forming sub-unit IIa. Compared to the lithology of the sediment cores, some of the stronger reflectors within seismic sub-unit IIb correspond to sandy-gravelly lenses (colored blue in Figure 3), whereas more chaotic layers represent gray clayey sediments with little or no structure, but ice rafted debris and shell fragments (Hannesdóttir, 2006). The boundary between seismic sub-units IIb and IIIa is channelized and reflects an erosional surface.

Seismic sub-unit IIIa is acoustically more distinctly stratified than the underlying seismic unit II. It can be traced throughout both basins although it has variable thickness. It is over 4 m thick at core site HST03-2A in the north basin (Table 3), whereas at core site HST03-1A in the south basin it is only about 1 m thick. This unit is thickest towards the southern part of seismic lines in the north basin, and in the middle part of seismic lines in the south basin (Figures 3 and 4). A comparison with the lithology of the two cores (1A and 2A) shows multiple graded sequences interbedded with finely laminated sediments.

Table 3. Thickness and volume of seismic units from the two sub-basins. Sedimentation rate for the various seismic units is calculated as far back as the chronological control reaches from the sediment cores. Since seismic unit I is only found scattered in the north basin, its thickness is included in thickness and volume numbers of seismic unit II. – *Þykkt og rúmmál seteininga úr báðum dældum vatnsins. Setmyndunarhraði ólíkra eininga er reiknaður eins langt aftur og aldursgreiningar leyfa. Þar eð eining I er einungis óreglulega dreifð í norðurdæld vatnsins er hún reiknuð sem hluti af einingu II hér.*

	Mean thickness (m)	Volume (km^3x10^{-3}) mean	max	Sed. rate cm/yr
North basin	(0.52 km^2)			
seismic unit IIIb	7.6±0.7	10.1	4.0	0.08
seismic unit IIIa	3.1±0.7	4.9	1.6	0.37
seismic unit II (a+b)	15.5±3.1	25.0	8.1	1.45
South basin	(0.28 km^2)			
seismic unit IIIb	6.4±1.2	9.1	1.8	0.06
seismic unit IIIa	2.1±0.6	3.6	0.6	0.21
seismic unit II (a+b)	19.2±5.9	34.7	5.4	0.45

The uppermost seismic sub-unit IIIb displays in most seismic profiles numerous regular, internal horizontal reflectors, typically more reflective than the underlying units, which compared to the core lithofacies represent abundant tephra layers and finely laminated, organic rich sediment. This unit is on average 11 m

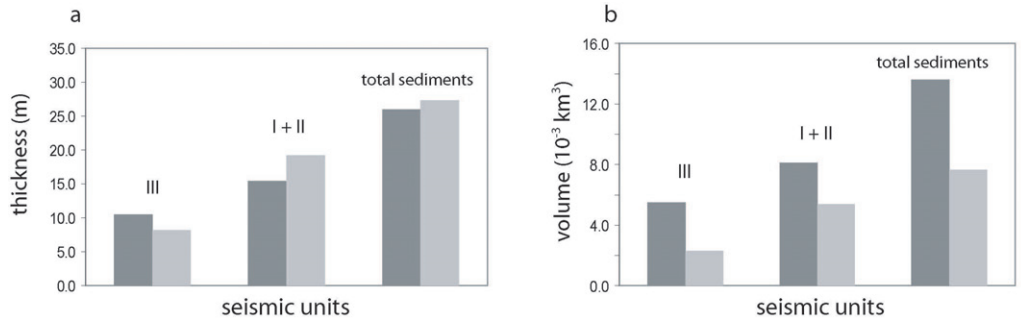

Figure 6. Mean thickness and volume of seismic units within specified depocenters (where total sediment thickness >20 m). North Basin sediments indicated in dark grey, South Basin sediments in light grey. a. Mean thickness of seismic units. b. Volume of the same seismic units. *– Meðalþykkt og rúmmál seteininga innan suður- og norðurdældar (skilgreint svæði þar sem setþykkt >20 m). Einingar í norðurdæld dökkgráar og í suðurdæld ljósgráar. a. Meðalþykkt seteininga. b. Reiknað rúmmál seteininga.*

thick in the north basin, with a maximum thickness of 13 m, but on average 8 m thick in the south basin and maximum of 11.5 m (Table 3).

Isopach maps of seismic units in Hestvatn and multibeam bathymetric map

Sedimentation accumulation rates (SAR) are given in Table 2 for the seismic units, except for the lowermost sediments (Figures 3 and 4). The highest SAR is observed in the marine sediments of seismic unit II. Seismic sub-unit IIIa corresponding to multiple graded sequences has twice the SAR in the north basin compared to the south. A more even SAR between the two sub-basins is recorded in seismic sub-unit IIIb, which also possesses the lowest SAR of the sedimentary record (Table 3).

The isopach maps, based on the identification of seismic units from Hestvatn sediments, suggest that the different sediment deposition between the two sub-basins is mostly controlled by past and present hydrology of the watershed and the landscape of the lake basin, including the narrow channel between the south and north basin (Figure 2). Isopach maps of total sediment for the whole lake show thickest sediment in the south basin (44 m) with a little over 30 m in the north basin (Figure 5). Volume and thickness calculations for the seismic units were confined to specified areas within the two basins, where total thickness is >20 m (Table 3). Seismic unit II makes up half of this thickness, or 19 m on average with maximum of 35 m. In the north basin it is 16 m on average with maximum thickness of 25 m (Figure 6a). However, due to the south basin's smaller size compared to the north, the volume is substantially less (Figure 6b). Seismic sub-unit IIIa is thicker in the north basin than the south basin. The unit shows a thickening towards the southern parts of the seismic lines in the north basin but it is thickest in the middle of the seismic lines in the south basin (Figures 3 and 4). If the axis of maximum thickness is followed from the north basin to the south basin it points to a source around the inlet of Krákulækur (Figure 1b). Seismic sub-unit IIIb is also considerably thicker in the north basin compared to the south basin (Figure 6a). This sedimentation pattern is probably related to the sediment source becoming restricted to a northern inlet- although it is also possible that the narrow channel connecting the two basins limited sediment delivery to the southern basin to suspended load sediment only. Paleobathymetric maps of the lake illustrating the configuration of the basin prior to any sediment deposition, and prior to deposition of seismic sub-unit IIIb (Figure 7) show that the bathymetry, after deposition of unit II, resembled modern-day bathymetry; the lake floor had been leveled out and the basins widened.

Various features of the bottom sediments are visible from the multibeam map revealing sediment forms and transport pathways hitherto unknown (Figure 2b). A distinctive platform is seen in the southwestern part

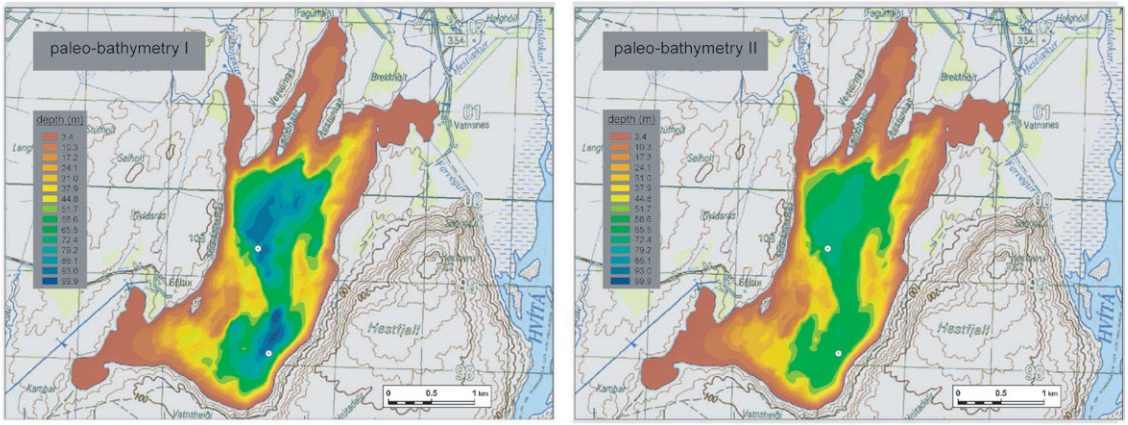

Figure 7. Paleobathymetry of Hestvatn. Paleobathymetry I depicts the configuration of the basin prior to any sediment infill. Paleobathymetry II shows the basin after seismic unit II is deposited. Both are superimposed on a subareal map, published with permission from the National Land Survey of Iceland. – *Dýptarkort af Hestvatni á mismunandi tímum. Mynd I sýnir botn vatnsins áður en nokkurt set hefur sest til. Mynd II sýnir botninn eftir að eining II hefur sest til. Landakort er birt með leyfi Landmælinga Íslands.*

of the south basin, protruding into the basin from the lake shore. Evidently sediment accumulation occurs in this cove of the lake, with transport from the west to the deepest part of the south basin. An apparent delta is observed at the mouth of Krákulækur (Figure 2b), where there is only minimal inflow today. A vague deltaic form (or sediment pile) is also visible in front of the middle cove at the north side of the lake. Small fan-like structures are observed along the steep bedrock walls on the eastern side of the lake. Multiple ridges are found in the area dividing the north and south basins of the lake, protruding up from the otherwise relatively flat lake bottom, thus narrowing the channel between the basins (Figure 2b).

INTERPRETATION

All but one seismostratigraphic unit (I) can be mapped across the Hestvatn basin and isopach maps of sediment thickness for each unit, derived using GIS software, show that sediment is not uniformly distributed across the lake basin. Seismic unit I is only found in a few of the lines from the north basin. From the acoustic character of seismic unit I and its small core sample we interpret this unit to be till. Since it is not possible to create a separate isopach map for seismic unit I it is combined with seismic unit II for the pertinent isopach map. These maps imply substantial changes in the dominant sediment sources from the deglaciation (seismic units I and II) and through the Holocene (seismic unit III).

Comparison of lithofacies and acoustic characteristics for seismic unit II in the south basin show the glaciomarine origin of the unit. The sediments were deposited in the submerged south basin before and during the deposition of the Vedde Ash, which is only found in the south basin. The till unit (seismic unit I) found in the north basin suggests occupation of the north basin by an outlet glacier at the time of the Vedde Ash formation. At this time most of seismic sub-unit IIa, was deposited in the south basin, explaining the thicker accumulation in that basin compared to the north basin. The fact that this seismic sub-unit IIa is only found in parts of the easternmost lying seismic line of the north basin (lies along the drumlin-like ridges), suggests that the accumulation took place during the retreating phase of the glacier that formed seismic unit I. Sediment accumulation rates for the seismic units show rapid sediment delivery during the marine depositional phase (Table 3). The transitional change from sub-unit IIa to sub-unit

IIb, reflects changes in sedimentary environment. Retreat of the ice lobe from the north basin was first followed by a marine transgression of that basin and deposition of glacial marine sediment of similar affinity as seismic sub-unit IIb in the south basin (Figure 8).

Continuing isostatic rebound resulted in isolation of the lake basin from the sea, dated to 10.6 ka BP (Hannesdóttir, 2006). Subsequently sediments accumulated in a freshwater system. Diatom analyses as well as changes in sediment lithology support this interpretation.

The strong irregular seismic reflector that separates seismic sub-unit IIb and the overlying acoustically well-stratified seismic sub-unit IIIa indicates an erosional event. When compared with core lithofacies of both cores (Hannesdóttir, 2006), seismic sub-unit IIIa marks a series of rhythmic units, each starting with coarse silt which grades into a clay cap. The rhythmites are separated by finely laminated grayish sediments. Seismic sub-unit IIIa is twice as thick in the north basin as in the south basin, and sediment accumulation rates are close to what is observed in the marine section (Table 3). We interpret these rhythmic sediments as turbidites, reflecting episodic sedimentation. In some areas, the turbidites eroded the underlying marine seismic unit II, resulting in the channelized boundary between the two units. The axes of channels and the maximum thickness of this unit points to a source through the Krákulækur inlet, which also could explain the relict form of a delta mouthing that inlet (Figure 2b).

The transition from seismic sub-unit IIIa to the overlying seismic sub-unit IIIb is indistinct in the seismic sections but very distinct in the sediment cores from both basins, which probably reflects small density differences in the fine grained graded sediment. Deposition of the Saksunarvatn Ash occurred just prior to the transition from seismic sub-units IIIa to IIIb (Jóhannsdóttir, 2007) (Figures 3 and 4). The well stratified appearance of sub-unit IIIb and the organic rich sediments revealed by the sediment cores from both basins indicate that Hestvatn reached a new equilibrium as a freshwater system. Sediment accumulation rates are the lowest for this seismic unit, showing the decreasing glacial influence on the sediment supply to the lake.

The multibeam map reveals important sedimentary features, which reflect changes in sediment envi-

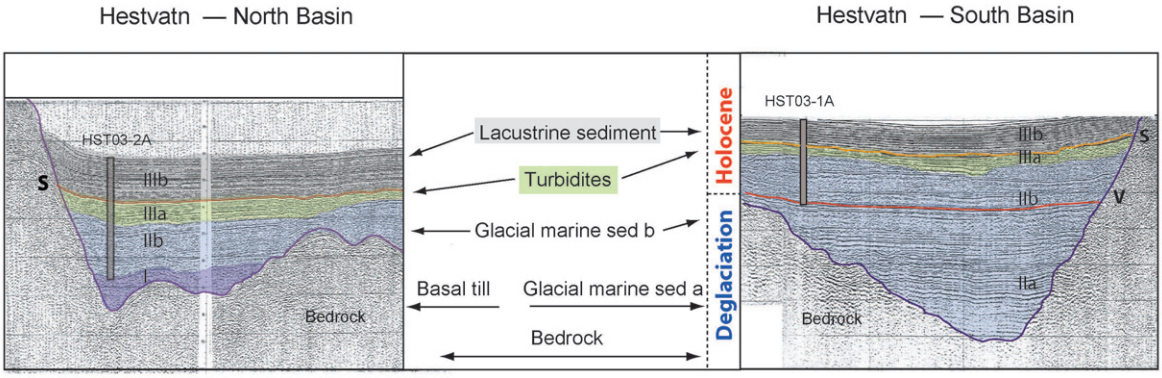

Figure 8. Seismic profiles containing the core sites from the north and south basins. The different pattern of the earliest sedimentation of the two basins is evident, with seismic unit I only present in the north basin, and thick seismic unit IIa characteristic of the south basin sediments. The north basin holds a thicker lacustrine sequence, because sediment delivery was restricted then to the northern basin. *– Endurvarpslínur sýna kjarnatökustaði í norður- og suðurdæld. Mismunandi setmyndun í neðstu setlögum Hestvatns er greinileg, þar sem eining I finnst einungis í norðurhluta vatnsins og þykk eining IIa er einkennandi í suðurhluta vatnsins. Stöðuvatnaset er mun þykkara í norðurdældinni, þar eð setflutningar voru aðallega frá lækjum á norðurströnd vatnsins.*

ronment and delivery paths to the lake. The multiple ridges between the north and south basins form possible pinning points for the calving glacier terminating in the paleobay west of Hestfjall. This position of the glacier terminus explains the thick glacio-marine sediments only found in the south basin of the lake. In the southwestern part of the south basin a platform extends into the lake from the shore, possibly related to the delta on the south shore of the lake (Figure 1b). The delta probably formed in front of a glacier tongue that curved around Hestfjall into the paleomarine environment during the accumulation of seismic sub-unit IIa. The fan-like structure at the mouth of Krákulækur, is the only profound deltaic feature in the north basin. This correlates with the thickness distribution of seismic sub-unit IIIa, which axis of maximum thickness points to a source around the inlet of Krákulækur. This may possibly have been the main inflow for the sediment-laden water forming the turbidites of seismic sub-unit IIIa.

DISCUSSION

A dynamic environment from a marine to a lacustrine sedimentation

The sediment record preserved in Hestvatn reflects a dynamic environment, which suggests a balance between glacial, marine and fluvial processes. The isopach maps of the seismic units demonstrate a shift of the main sediment pathways to the lake basin. Differences in the seismic units' spatial distribution reflect changes in the sediment source, mainly affected by deglaciation and the subsequent isostatic rebound, isolating the lake basin from the sea. The new sediment cores reveal a succession of turbidites (seismic unit IIIa, hitherto unrecovered from Hestvatn), which allow re-interpretation of the seismic data. The associated seismic unit has a clear lower boundary - an erosional surface, and was deposited during an interval of only 600 years (Hannesdóttir, 2006).

The seismic survey and the isopach maps of seismic units I and II demonstrate an environment dominated by a tidewater glacier that was pinned between the two sub-basins. Although the tidewater glacier in the north basin delivered substantial sediment to the southern basin, a sandy-gravelly ice-contact marine delta at the south end of the lake graded to 50 m a. s. l. suggests that some of the gravelly layers of seismic unit II in the south basin may have been sourced from another glacier tongue that curved around the east side of Hestfjall. This interpretation is supported by the platform in the southwest part of the south basin on the multibeam map. Longshore drift may have also contributed a substantial volume of sediment to the south basin prior to isolation from the sea. Changes within seismic unit II indicate retreat of the glacier and subsequent isolation of Hestvatn as it changed into a lacustrine environment. A shift in sediment source is evident from the isopach maps, with the primary locus of sedimentation shifting from the south basin to the north basin as deglaciation progressed (Figures 5 and 6). A succession of thick, distinctly graded sedimentary units interbedded with finely laminated sediment reflects the episodic input of turbidites associated with failures of ice dams up stream of Hestvatn. The timing of these turbidites coincides with the retreat of the main Iceland Ice Sheet from the Kjölur highland area $\sim$80 km north of the Hestvatn basin (Figure 1a) and suggests their origin to be the results of repeated release of ice-dammed lakes (Kjartansson, 1964; Tómasson, 1993; Kaldal and Víkingsson, 1990). The turbidites were deposited as jökulhlaups in the newly established lake, and are not observed in the marine section of the sedimentary record. However, the preservation potential of flood deposits entering the sea is not high for modern day jökulhlaups (e.g. Maria *et al.*, 2000), and jökulhlaups prior to isolation of Hestvatn may not be apparent.

Isolation of the lake basin provides information on glacial rebound during last deglaciation. The rapid change in diatom flora from marine to freshwater assemblages, recorded in the sediment cores (Hannesdóttir, 2006), indicate rapid uplift, in accordance with the sensitivity of the Icelandic crust to glacial loading and unloading (Sigmundsson, 2006). According to lithological and diatom analysis the Hestvatn basin became isolated around 10.6 ka, hence sea level was at that time 50 m a. s. l. This data point adds to a set of a few dated sea level stands in south Iceland (Hjartarson, 1988; Hjartarson and Ingólfsson, 1988; Geirs-

dóttir *et al.*, 1997). The Hestvatn sedimentary record is the only archive where the isolation contact (transition from marine to a terrestrial environment) in South Iceland has been dated.

The uppermost seismic sub-unit IIIb with the very fine acoustic reflectors matching tephra layers in the sediment cores reflects sedimentation in a freshwater system. Most of the sediment of this unit was formed from a suspended load, which also results in a much better preservation of tephra layers than in the underlying seismic units. The multibeam bathymetric map reflects the most recent conditions in Hestvatn. Relict geomorphic structures are thought to reflect sedimentation during earlier times.

Implication for the deglacial history of the southern lowlands of Iceland and correlation with the North Atlantic region

Different views on the size of the Younger Dryas glacier in South Iceland have been suggested. Kjartansson (1939) described a limited Late Weichselian ice sheet, with thin lobate glaciers from the highlands, following the modern river courses of Hvítá and Þjórsá. A heavy Younger Dryas glaciation of South Iceland was inferred by Hjartarson and Ingólfsson (1988) and Hjartarson (1991) based on deficit of shells of Allerød age in the southern lowlands. Geirsdóttir *et al.* (2000) argued a more limited Younger Dryas glaciation based on research of the Búði moraines and lacustrine studies from South Iceland (also Harðardóttir *et al.*, 2001a). Re-interpreted seismic data and multibeam images from Hestvatn have revealed a dynamic depositional environment during the deglaciation of the southern lowlands.

The occurrence of glacial deposits in the north sub-basin of Hestvatn and the restriction of the Vedde Ash to the marine sediments in the south-basin, indicates that during Younger Dryas time (12.7–11.5 ka) outlet glaciers in southern Iceland terminated in a marine embayment inland from the current coastline, at or just beyond the Búði moraines in southern

Figure 9. Possible position of ice margin at various times during Younger Dryas, deglaciation and Early Holocene derived from available data. Images based on Digital Elevation Maps (http://edcdaac.usgs.gov), with a resolution of about 1 km per grid cell. Glacial striations are marked with black lines and fluted moraines with blue lines (Kaldal and Víkingsson, 1990). A. Younger Dryas glacier terminating in Hestvatn (∼12.0 cal. kyr BP), various evidence of the glacier terminating in the north basin of Hestvatn (see text). B. Búði morainal complex (∼11.0 cal. kyr BP), the configuration of the moraines (orange) is from Kjartansson (1939), Hjartarson and Ingólfsson (1988) Geirsdóttir *et al.* (1997), and evidence of ice-marginal lakes is from Áskelsson (1942), Kjartansson (1964), Tómasson (1993), and Geirsdóttir *et al.* (2000). Red dots are sections with jökulhlaup deposits mapped by Axelsdóttir (2005). C. Isolation of Hestvatn and jökulhlaups (∼10.6 cal. kyr BP). Extent of ice-dammed lakes based on measurements by Tómasson (1993), end-moraines mapped by Kaldal and Víkingsson (1990). D. Early Holocene (∼10.0 cal. kyr BP), glacier retreating towards the mountainous area in SE Iceland, most of the highlands ice free. – *Möguleg staða ísaldarjökulsins á mismunandi tímum frá Yngra Dryas til upphafs Nútíma byggt á margvíslegum gögnum. Grunnmyndir frá http://edcdaac.usgs.gov með 1 km upplausn. Jökulrákir merktar með svörtum línum og jökulgarðar með bláum línum (Ingibjörg Kaldal and Skúli Víkingsson, 1990). A. Yngri Dryas jökullinn kelfir í Hestvatni (sjá texta). B. Búðagarðarnir (um 11.000 ára gamlir) sýndir á einfaldan hátt með appelsínugulum línum samkvæmt Guðmundi Kjartanssyni (1939) og Árna Hjartarsyni og Ólafi Ingólfssyni (1988), Áslaugu Geirsdóttur o. fl. (1997). Gögn um jökulstífluð vötn eru fengin frá Jóhannesi Áskelssyni (1942), Guðmundi Kjartanssyni (1964), Hauki Tómassyni (1993), og Áslaugu Geirsdóttur o. fl. (2000). Rauðir punktar tákna opnur þar sem jökulhlaupaset hefur verið kortlagt (Hulda Axelsdóttir, 2005). C. Einangrun Hestvatns og fyrstu jökulhlaup (um 10.600 ár). Jökulstífluð vötn á Kili eru teiknuð samkvæmt mælingum frá Hauki Tómassyni (1993), jökulgarðar eftir Skúla Víkingssyni og Ingibjörgu Kaldal (1990). D. Upphaf Nútíma (10.000 ár) og jökullinn hörfar inn til landsins. Á þessum tíma er mestur hluti hálendisins orðinn jökullaus.*

Iceland. One ice lobe occupied the northern basin of Hestvatn where bedrock ridges bordering and within the narrow channel between the two sub-basins (Figure 8). provided pinning points that stabilized the ice margin (Figure 9). The outlet glacier terminating in the north basin contributed sediment to the submerged south basin (seismic sub-unit IIa; Figure 8). A second lobe flowed around the east side of Hestfjall, depositing a delta at the SE shore of the lake, and adding to the sediment accumulation in the south basin (Fig-

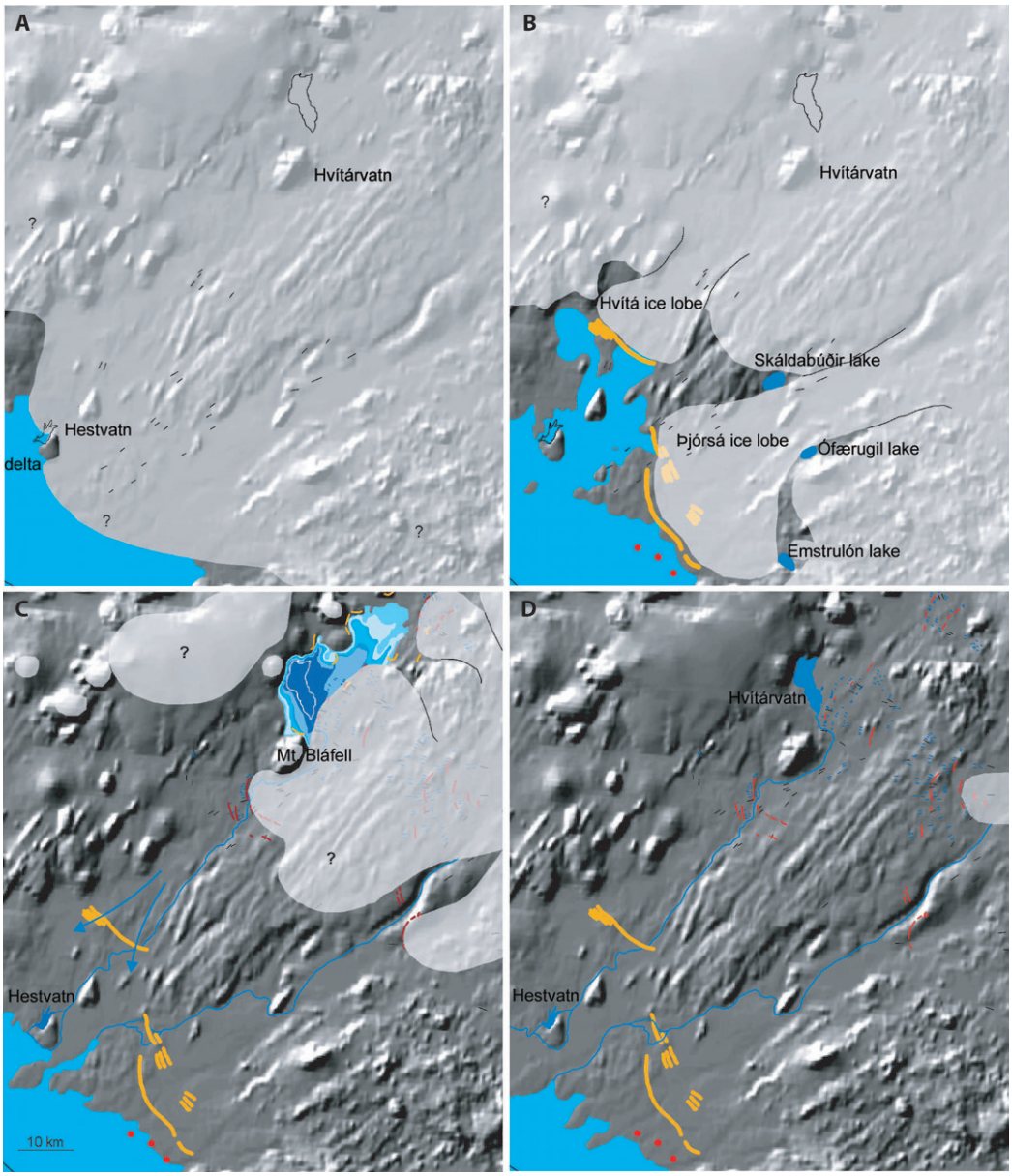

ure 9). This provides a more detailed picture of the structure of the Younger Dryas glacier in South Iceland than previously shown (Geirsdóttir *et al.*, 1997, 2000; Harðardóttir *et al.*, 2001a; Norðdahl and Pétursson, 2005) (Figure 9).

The North Atlantic region experienced a series of abrupt climatic changes during the Pleistocene-Holocene transition (e.g. Bradley *et al.*, 2002). The two most prominent being the Younger Dryas dated to 12.9–11.7 ka (Rasmussen *et al.*, 2006) in the GRIP ice core record and the Preboreal Oscillation beginning at 11.5 ka (Rasmussen *et al.*, 2007). The temperature oscillations have been related to variable strength of the thermohaline circulation of the North Atlantic, influenced by increased freshwater input (e.g. Mercer, 1969; Broecker *et al.*, 1989; Koc Karpuz and Jansen, 1992; Björck *et al.*, 1996; Clark *et al.*, 2001; Broecker, 2003). Former ice-marginal lakes are known from both sides of the North Atlantic and outbursts of various freshwater sources have been suggested to cause the Younger Dryas and Preboreal cooling (e.g. Broecker *et al.*, 1989; Keigwin *et al.*, 1991; Sarnthein *et al.*, 1995; Hald and Hagen, 1998; Teller, 2002; Jennings *et al.*, 2006).

The jökulhlaups entered Hestvatn during a 600 year period between 10.6 and 10.0 ka, which is a few hundred years after the termination of the Pre-Boreal Oscillation. Did jökulhlaups flow into the paleobay of the southern lowlands before that time? Jökulhlaup activity during deglaciation of South Iceland has been reported from a number of sites (Geirsdóttir *et al.*, 1997, 2000; Jennings *et al.*, 2000). Lacasse et al. (1996) find turbidites in marine sediment cores on the south Iceland shelf, which they assign to jökulhlaup activity following volcanic or glacial events occurring in southern Iceland during the last two glaciations and the early Holocene. As mentioned before, the preservation potential in a marine setting is not as good as in the lacustrine environment due to several factors. Jökulhlaups do not form underflows as easily in salty water, bioturbation results in homogeneous mud, and jökulhlaup deposits are hard to distinguish from sediments deposited in front of a calving glacier as was the case in the south basin of Hestvatn. We can therefore not rule out the possibility that jökulhlaups entered the Hestvatn site prior to 10.6 ka BP, although they are not distinguished in the marine sedimentary record. However, our record in the Hestvatn basin suggests repeated jökulhlaups during the retreat of the Iceland ice cap from the central highlands with major routes towards south. The volume of the jökulhlaups originating north of Hestvatn probably was too small to cause significant changes in the thermohaline circulation of the North Atlantic. Due to the proximity to the formation site of North Atlantic Deep Water, deglacial jökulhlaups in Iceland might have had a local impact on deep-water formation. However, their volume compared with meltwater released from e.g. Lake Agassiz during deglaciation (e.g. Teller *et al.*, 2002; Clarke *et al.*, 2004) is minimal. The turbidite record of the Hestvatn cores provides us with a more detailed picture of the deglacial environment in the southern lowlands of Iceland.

CONCLUSION

The new sediment cores from Hestvatn, re-evaluation of seismic profiles and a multibeam survey provide new insight to the deglaciation of the southern lowlands of Iceland. Interpretation of more than 100 km of seismic reflection profiles of bottom sediments in lake Hestvatn, South Iceland, reveals two sub-basins filled with up to 44 m of deglacial and Holocene sediments. Together with sediment cores retrieved from both basins, a major change in sedimentary environments from glacial marine to lacustrine sedimentation is observed. Implications for Younger Dryas glacier extent are derived from the surveys and sediment cores, suggesting that during deglaciation the northern basin was occupied by an outlet glacier whereas the southern basin accumulated glacial marine sediments. Glacial retreat is observed in the marine record, followed by isostatic rebound that lead to isolation of the lake basin around 10.6 ka. This provides important information on relative sea level change and glacial rebound. Erosional surfaces are seen at the boundary of marine and lacustrine sediments, on top of which sequence of turbidites are deposited, thought to reflect episodic sedimentation, related to jökulhlaups during the deglaciation.

Acknowledgements

A RANNIS Grant of Excellence from the Icelandic Centre of Research to Á. G. and G. H. M. for the project Warm times-cold times, and the US National Science Foundation (OPP-0138010) provided support for most of the field and analytical work included in this study. The Icelandic Centre for Research supported H. H. via a Student Research Grant (Rannsóknanámssjóður RANNIS). The University of Arizona is thanked for radiocarbon dates. Finnur Pálsson, Eyjólfur Magnússon and Þórdís Högnadóttir are thanked for their help digitizing the seismic data. We thank everyone who helped during the GLAD 2000 coring operation in 2003, especially Þorsteinn Jónsson and Sveinbjörn Steinþórsson. Authors acknowledge two anonymous reviewers.

Setlög á botni Hestvatns

Meira en 100 km af endurvarpsgögnum ásamt fjölgeislamælingum af setlögum á botni Hestvatns á Suðurlandi, sýna tvær dældir með 44 m þykkum setlögum frá síðjökultíma og Nútíma. Aldur setlaganna er fenginn með gjóskulögum og geislakolsmælingum á skeljum úr sjávarsetinu. Vedde og Saksunarvatn gjóskulögin veita mikilvægar upplýsingar um röð atburða á síðjökultíma. Fimm seteiningar eru skilgreindar samkvæmt endurvarpsgögnunum ásamt upplýsingum úr setkjörnum úr báðum dældum vatnsins. Setlögin sýna breytingar sem verða í setmyndun í vatninu frá jökul- og jökulsjávar- til stöðuvatnaumhverfis. Jafnþykktarkort sýna hvernig setuppbyggingu er háttað á ákveðnum tímabilum og breytingar sem verða í setmyndun í norður- og suðurhluta vatnsins. Vedde gjóskulagið finnst einungis í jökulsjávarsetinu í suðurdæld vatnsins, sem bendir til þess að Yngri Dryas jökullinn hafi náð út í norðurdæld vatnsins og skilað af sér seti í suðurhluta þess. Háupplausnar fjölgeislamælingar á botni Hestvatns sýna fjöldann allan af lágum hryggjum á svæðinu sem skilur að dældirnar tvær, en þar hefur jökullinn líklega byrjað að kelfa. Eftir hörfun jökulsins og einangrun vatnsins hófst myndun stöðuvatnasets, sem er aðallega komið úr lækjum á norður- og norðvesturhlið vatnsins, sem leiðir til meiri setupphleðslu í norðurhluta vatnsins. Jökulhlaupaset er í neðstu lögum stöðuvatnasetsins, talið eiga uppruna sinn í jökulstífluðum vötnum við jaðar hörfandi ísaldarjökulsins á miðhálendinu.

REFERENCES

Andrews, J. T., J. Harðardóttir, G. Helgadóttir, A. Jennings, Á. Geirsdóttir, Á. E. Sveinbjörnsdóttir, S. Schoolfield, G. B. Kristjánsdóttir, L. M. Smith, K. Thors and J. P. M. Syvitski 2000. The N and W Iceland shelf: insights into Last Glacial Maximum ice extent and deglaciation based on acoustic stratigraphy and basal radiocarbon AMS dates. *Quaternary Sci. Rev.* 19, 619–631.

Andrews, J. T. and G. Helgadottir 2003. Late Quaternary ice cap extent and deglaciation, Hunafloaall, Northwest Iceland: Evidence from marine cores. *Arctic, Antarctic and Alpine Res.* 35, 218–232.

Axelsdóttir, H. 2005. *Myndun og mótun Rangárvalla, landform og setmyndunarumhverfi*. Unpublished M. Sc. Thesis, University of Iceland, Reykjavík, 97 pp.

Áskelsson, J. 1942. Jarðfræði og jarðmyndun. *In:* Eyþórsson, J. (ed.), *Árbók Ferðafélags Íslands 1942. Kerlingarfjöll*. Ferðafélag Íslands, Reykjavík, 22–29.

Bard, E., M. Arnold, J. Mangerud, M. Paterne, L. Labeyrie, J. Duprat, M-A. Melieres, E. Sønstegaard and J-C. Duplessy 1994. The North Atlantic atmosphere-sea surface ^{14}C gradient during the Younger Dryas climate event. *Earth Planet. Sci. Lett.* 126, 275–287.

Becker, B., B. Kromer and P. Trimborn 1991. A stable isotope tree-ring timescale of the Late Glacial/Holocene boundary. *Nature* 353, 647–649.

Björck, S., B. Kromer, S. J. Johnsen, O. Bennike, D. Hammarlund, G. Lemdahl, G. Possnert, T. L. Rasmussen, B. Wohlfarth, C. U. Hammer and M. Spurk 1996. Synchronized terrestrial atmospheric deglacial records around the North Atlantic. *Science* 274, 1155–1160.

Bradley, R. S., K. R. Briffa, J. Cole, M. K. Hughes and T. J. Osborn 2002. The climate of the last millennium. *In:* Alverson, K. D., R. S. Bradley and T. F. Pedersen (eds.), *Paleoclimate, Global Change and the Future*. Springer, Heidelberg, 105–141.

Broecker, W. S., J. P. Kennett, B. P. Flower, J. T. Teller, S. Trumbore, G. Bonani and W. Wolfli 1989. Routing of meltwater from the Laurentide Ice Sheet during the Younger Dryas cold episode. *Nature* 341, 318–321.

Brocker, W. S., 2003. Does the trigger for abrupt climate change reside in the ocean or in the atmosphere? *Science* 300, 1519–1522.

Clark, P. U., S. J. Marshall, G. K. C. Clarke, S. W. Hostetler, J. M. Licciardi and J. T. Teller 2001. Freshwater forcing of abrupt climate change during the last glaciation. *Science* 293, 283–287.

Clarke, G. K. C., D. W. Leverington, J. T. Teller and A. S. and Dyke 2004. Paleohydraulics of the last outburst flood from glacial lake Agassiz and the 8200 BP cold event. *Quaternary Sci. Rev.* 23, 389–407.

Dugmore, A. J., G. T. Cook, J. S. Shore, A. J. Newton, K. J. Edwards and G. Larsen 1995. Radiocarbon dating of tephra layers in Britain and Iceland. *Radiocarbon* 37, 379–388.

Geirsdóttir, Á., J. Eiríksson, J. and Harðardóttir 1997. The depositional history of the Younger Dryas-Preboreal Búdi moraines in south-central Iceland. *Arctic and Alpine Res.* 29, 13–23.

Geirsdóttir, Á., J. Hardardóttir and A. E. Sveinbjörnsdóttir 2000. Glacial extent and catastrophic meltwater events during the deglaciation of Southern Iceland. *Quaternary Sci. Rev.* 19, 1749–1761.

Geirsdóttir, Á., J. Andrews, S. Ólafsdóttir, G. Helgadóttir and J. Harðardóttir 2002. A 36 Ky record of iceberg rafting and sedimentation from north-west Iceland. *Polar Res.* 21, 291–298.

Geirsdóttir, Á., G. H. Miller and J. T. Andrews 2007. Glaciation, erosion, and landscape evolution of Iceland. *J. Geodynamics* 43, 170-Ű186.

Geirsdóttir, Á., G. H. Miller, Y. Axford and S. Ólafsdóttir 2009. Holocene and latest Pleistocene climate and glacier fluctuations in Iceland. *Quaternary Sci. Rev.* 28, 2107–2118.

Glew, J. R. 1991. Miniature gravity corer for recovering short sediment cores. *J. Paleolimnology* 5, 285–287.

Grönvold, K., N. Óskarsson, S. J. Johnsen, H. B. Clausen, C. U. Hammer, G. Bond and E. Bard 1995. Tephra layers from Iceland in the Greenland GRIP ice core correlated with oceanic and land sediments. *Earth Planet. Sci. Lett.* 135, 149–155.

Haflidason, H., H. P. Sejrup, K. Klitgaard Kristensen and S. Johnsen 1995. Coupled response of the late glacial climatic shifts of northwest Europe reflected in Greenland ice cores: evidence from the northern North Sea. *Geology* 23, 1059–1062.

Hald, M. and S. Hagen 1998. Early Preboreal cooling in the Nordic seas region triggered by meltwater. *Geology* 26, 615–618.

Hannesdóttir, H. 2006. *Reconstructing environmental change in South Iceland during the last 12, 000 years-based on sedimentological and seismostratigraphical studies in lake Hestvatn*. Unpublished M. Sc. thesis, University of Iceland, Reykjavík.

Harðardóttir, J., Á. Geirsdóttir and Á. E. Sveinbjörnsdóttir 2001a. Seismostratigraphy and sediment studies of Lake Hestvatn, southern Iceland: implications for the deglacial history of the region. *J. Quaternary Sci.* 16, 167–179.

Harðardóttir, J., Á. Geirsdóttir and Þ. Þórðarson 2001b. Tephra layers in a sediment cores from Lake Hestvatn, southern Iceland: implications for evaluating sedimentation processes and environmental impacts on a lacustrine system caused by tephra fall deposits in the surrounding watershed. *Spec. Publs. Int. Ass. Sed.* 30, 225–246.

Hjartarson, Á. 1988. Þjórsárhraunið mikla, stærsta nútímahraun jarðar. *Náttúrufræðingurinn* 58, 1–16.

Hjartarson, Á. 1991. A revised model of Weichselian deglaciation in South and Southwest Iceland. *In:* Maizels, J. K. and C. Caseldine (eds.), *Environmental Change in Iceland: Past and Present*. Kluwer Academic Press, Netherlands, 67–77.

Hjartarson, Á. and Ó. Ingólfsson 1988. Preboreal glaciation of southern Iceland. *Jökull* 38, 1–16.

Ingólfsson, Ó. and H. Norðdahl 1994. A review of the environmental history of Iceland, 13000–9000 yr BP. *J. Quaternary Sci.* 9, 147–150.

Ingólfsson, Ó. and H. Norðdahl 2001. High relative sea level during the Bølling interstadial in western Iceland: a reflection of ice-sheet collapse and extremely rapid glacial unloading. *Arctic, Antarctic and Alpine Res.* 33, 231–243.

Jakobsson, S. P., J. Jónsson and F. Shido 1978. Petrology of the western Reykjanes Peninsula, Iceland. *J. Petrology* 19, 669–705.

Jennings, A., J. Syvitsky, L. Gerson, K. Grönvold, Á. Geirsdóttir, J. Harðardóttir, J. Andrews and S. Hagen 2000. Chronology and paleoenvironments during the late Weichselian deglaciation of the southwest Iceland shelf. *Boreas* 29, 167–193.

Jennings, A., M. Hald, M. Smith and J. T. Andrews 2006. Freshwater forcing from the Greenland Ice Sheet during the Younger Dryas: evidence from southeastern Greenland shelf cores. *Quaternary Sci. Rev.* 25, 282–298.

Jóhannsdóttir, G. E. 2007. *Mid-Holocene to late glacial tephrochronology in West Iceland as revealed in three*

lacustrine environments. Unpublished M. Sc. thesis, University of Iceland, Reykjavík, 169 pp.

Jull, M. and D. McKenzie 1996.The effect of deglaciation on mantle melting beneath Iceland. *J. Geophys. Res.* 101, 21815–21828.

Kaldal, I. and S. Víkingsson 1990. Early Holocene deglaciation in central Iceland. *Jökull* 40, 51–66.

Keigwin, L. D., G. D. Jones and S. J. Lehman 1991. Deglacial meltwater discharge, North Atlantic deep circulation, and abrupt climate changes. *J. Geophys. Res.* 96, 16811–16826.

Kjartansson, G. 1939. Stadier i isens tilbagerykning fra det sydvestislandske lavland. *Medd. Dansk Geol. Forening* 9, 426–445.

Kjartansson, G. 1964. Ísaldarlok og eldfjöll á Kili. *Náttúrufræðingurinn* 34, 9–38.

Koc Karpuz, N. and E. Jansen 1992. A high-resolution diatom record of the last deglaciation from the SE Norwegian sea: documentation of rapid climatic changes. *Paleoceanography* 7, 499–520.

Kromer, B. and B. Becker 1993. German oak and pine ^{14}C calibration, 7200–9400 BC. *Radiocarbon* 35, 125–136.

Lacasse, C., S. Carey and H. Sigurdsson 1998. Volcanogenic sedimentation in the Iceland Basin: influence of subaerial and subglacial eruptions. *J. Volcanol. Geoth. Res.* 83, 47–73.

Lowe, J. J. and M. J. C. Walker 2000. Radiocarbon dating the last glacial-interglacial transition (ca. 14–9 ^{14}C ka BP) in terrestrial and marine records: the need for new quality assurance protocols. *Radiocarbon* 42, 53–68.

Maria, A., S. Carey, H. Sigurdsson, C. Kincaid and G. Helgadóttir 2000. Source and dispersal of jökulhlaup sediments discharged to the sea following the 1996 Vatnajökull eruption. *GSA Bulletin* 112, 1507–1521.

Mercer, J. H. 1969. The Alleröd oscillation: a European climatic anomaly? *Arctic and Alpine Res.* 1, 227–234.

Norðdahl, H. and H. G. Pétursson 2005. Relative sea-level changes in Iceland: new aspects of the Weichselian deglaciation in Iceland. *In:* Caseldine, C., A. J. Russell, J. Harðardóttir and Ó. Knudsen (eds.) *Iceland-Modern Processes and Past Environments*. Amsterdam, Elsevier, 25–78.

Rasmussen, S. O., *et al.* 2006. A new Greenland ice core chronology for the last glacial termination. *J. Geophys. Res.* 111, D06102, doi:10.1029/2005JD006079.

Rasmussen, S. O., B. M. Vinther, H. B. Clausen and K. K. Andersen 2007. Early Holocene climate oscillations recorded in three Greenland ice cores. *Quaternary Sci. Rev.* 26, 1907–1914.

Rist, S. 1975. Stöðuvötn. OS-vatn 7503/OS-ROD 7519. National Energy Authority, Reykjavík.

Róbertsdóttir, B. 1992. *Forsöguleg gjóskulög frá Kötlu, áður nefnd „Katla 5000“*. Geoscience Society of Iceland. Spring Meeting. Conference Proceedings.

Rundgren, M., Ó. Ingólfsson, S. Björck, H. Jiang and H. Haflidason 1997. Dynamic sea level change during the last deglaciation of northern Iceland. *Boreas* 20, 201–215.

Sarnthein, M., E. Jansen, M. Weinelt, M. Arnold, J. Claude Duplessy, H. Erlenkauser, A. Flatøy, G. Johannessen, T. Johannessen, S. Jung, N. Koc, L. Labeyrie, M. A. Maslin, U. Pflaumann and H. Schulz 1995. Variations in Atlantic surface ocean paleoceanography, 50–80° N: A time-slice record of the last 30,000 years. *Paleoceanography* 10, 1063–1094.

Sigbjarnarson, G. 1976. Hagafellsjökull eystri hlaupinn. The surge of Hagafellsjökull eystri. *Jökull* 26, 94–96.

Sigmundsson, F. 2006. Glacial isostasy and sea-level change: rapid vertical movements and changes in volcanic production rates. *Iceland Geodynamics- crustal deformation and divergent plate tectonics*. Springer, Berlin, 151–173.

Sigvaldason, G., K. Annertz and M. Nilsson 1992. Effect of glacier loading/deloading on volcanism: postglacial volcanic production rate of the Dyngjufjöll area, central Iceland. *Bull. Volc.* 54, 385–392.

Sinton, J., K. Grönvold and K. Sæmundsson 2005. Postglacial eruptive history of the Western Volcanic Zone, Iceland. *Geochem. Geophys. Geosystems* 6(Q12009, doi:10.1029/2005GC001021).

Stuvier, M. and P. J. Reimer 1993. Extended ^{14}C data base and revised CALIB 3.0 ^{14}C-calibration program. *Radiocarbon* 35, 215–230.

Stuvier, M., P. J. Reimer, E. Bard, J. W. Beck, G. S. Burr, K. A. Hughen, B. Kromer, G. McCormac, J. Van Der Plicht and M. Spurk 1998. INTCAL98 radiocarbon age calibration, 24,000-0 cal. BP. *Radiocarbon* 40, 1041–1083.

Sveinbjörnsdóttir, Á. E., Á. Geirsdóttir and J. Harðardóttir 1998. ^{14}C AMS dating of Icelandic lake sediments. *Radiocarbon* 40, 865–872.

Syvitski, J. P., A. E. Jennings and J. T. Andrews 1999. High-resolution seismic evidence for multiple glaciations across the Southwest Iceland shelf. *Arctic, Antarctic and Alpine Res.* 31, 50–57.

Teller, J. T., D. W. Leverington and J. D. Mann 2002. Freshwater outbursts to the oceans from glacial lake Agassiz and their role in climate change during the last deglaciation. *Quaternary Sci. Rev.* 21, 879–887.

Þórarinsson, S. 1975. Katla og annáll Kötlugosa. *Árbók Ferðafélags Íslands*, 124–129.

Tómasson, H. 1961. *Hestvatn hydro-electric project*. The State Electricity Authority, Reykjavík.

Tómasson, H. 1993. Jökulstífluð vötn á Kili og hamfarahlaup í Hvítá í Árnessýslu. *Náttúrufræðingurinn* 62, 77–98.

Hestfjall and Hestvatn viewed from the south, with Vörðufell in the background. The river Hvítá runs east of Hestfjall and westwards along the southern side of the Hestvatn lake. The freshwater input from Slauka (the only outflow of Hestvatn) blends in with the glacial water of Hvítá on the eastern side of Hestvatn. – *Horft til norðurs yfir Hestvatn og Hestfjall, Vörðufell sést í bakgrunni. Hvítá rennur austan Hestfjalls og beygir til vesturs suður með Hestvatni. Ferskvatnið frá Slauku blandast jökullitaðri Hvítánni austan megin við vatnið.* Photo/*ljósmynd*: Oddur Sigurðsson, October 30th, 1985.